

ANOMALOUS STABILITY OF $\nu = 1$ BILAYER QUANTUM HALL STATE

A. Sawada, Z.F. Ezawa, H. Ohno^a, Y. Horikoshi^b
O. Sugie, S. Kishimoto^a, F. Matsukura^a, Y. Ohno^a, M. Yasumoto
Department of Physics, Tohoku University, Sendai 980-77, Japan

^a *Research Institute of Electrical Communication, Tohoku University, Sendai 980-77, Japan*

^b *School of Science and Engineering, Waseda University, Tokyo 169, Japan*

We have studied the fractional and integer quantum Hall (QH) effects in a high-mobility double-layer two-dimensional electron system. We have compared the "stability" of the QH state in balanced and unbalanced double quantum wells. The behavior of the $\nu = 1$ QH state is found to be strikingly different from all others. It is anomalously stable, though all other states decay, as the electron density is made unbalanced between the two quantum wells. We interpret the peculiar features of the $\nu = 1$ state as the consequences of the interlayer quantum coherence developed spontaneously on the basis of the composite-boson picture.

I. INTRODUCTION

The bilayer quantum Hall (QH) system possesses a rich phase diagram [1] since it allows three controllable parameters, the magnetic length ℓ_B , the interlayer distance d and the symmetric-antisymmetric tunneling gap energy Δ_{SAS} . By controlling these parameters we can realize various bilayer QH states $\Psi_{m_f m_b m}$ with m_α odd integers and m an integer ($m_\alpha \geq m$) [2]. When the interlayer and intralayer Coulomb interactions becomes nearly equal, the Ψ_{mmm} state is realized at $\nu \equiv 1/m$. A novel interlayer quantum coherence (IQC) has been predicted to develop spontaneously in the Ψ_{mmm} states [3], which is characterized by a pseudo-gapless mode describing the interlayer phase and the electron density difference. A typical QH state is given by Ψ_{111} at $\nu = 1$. The $\nu = 1/m$ QH state is intriguing since there are two distinguishable states, the monolayer state stabilized by the tunneling interaction and the coherent state Ψ_{mmm} stabilized by the Coulomb interaction.

We wish to address what are the signals for the spontaneous development of IQC characterizing the Ψ_{mmm} state. Murphy *et al.* [4] made an experiment in which they observed an anomalous activation energy dependence of the $\nu = 1$ state on the tilted magnetic field, which is probably one of the signals [5,6]. Furthermore, their data indicate that IQC is observable even at a large tunneling interaction, $\Delta_{SAS} \approx 8.4\text{K}$.

In search for a clear signal we have performed an experiment on bilayer QH states by varying the density ratio of the two layers as well as the total electron density. We hereafter refer to the QH states as "balanced

QH states" when the densities are equal, and as "unbalanced QH states" when they are not equal. Experiments have so far been made extensively on balanced QH states [2,7], and only limited works have been done on the unbalanced QH states [8,9]. The study of unbalanced QH states reveals its character: For instance, if the QH state is stabilized by the energy gap Δ_{SAS} , it decays as the system becomes unbalanced.

In our experimental data, all QH states depend sensitively on the density ratio except the $\nu = 1$ state. They have strong tendency to decay as the electron density between the two quantum wells is made unbalanced.

On the contrary, the behavior of the $\nu = 1$ state is strikingly different from all others. The $\nu = 1$ state is stable even if the density ratio is changed, as far as the total density is less than a critical value. We interpret that this stability of the $\nu = 1$ state is an evidence of the IQC developed spontaneously.

II. EXPERIMENTAL RESULTS

The sample was grown by molecular beam epitaxy on (100)-oriented GaAs substrate, and consists of two modulation-doped 200 Å quantum wells, separated by $\text{Al}_{0.3}\text{Ga}_{0.7}\text{As}$ barriers of thickness $d_B = 31\text{Å}$. It has the total density $2.3 \times 10^{11}\text{cm}^{-2}$ and the mobility $3.0 \times 10^5\text{cm}^2/\text{Vs}$ at 30 mK at zero gate voltage. Measurements were performed with the sample mounted in the mixing chamber of a dilution refrigerator with a base temperature less than 6 mK. The maximum field of our superconducting magnet is 13.5 T at 4.2 K. Temperature was measured by a RuO_2 resistance set near the sample and calibrated by ^3He melting pressure thermometer. Standard low-frequency ac lock-in techniques were used with currents less than 100 nA to avoid heating effects.

Schottky front and back gates were used to change the total carrier density and the density ratio of the two quantum wells. In Fig.1 the densities n_f and n_b of the front and back layers were obtained from Fourier transforms of the low-field ($B < 1.3\text{T}$) Shubnikov-de Haas (SdH) oscillations, and the total density n_t was obtained from the Hall resistance at low fields. The sum of n_f and n_b is in good agreement with n_t obtained from the Hall resistance. We note the following features: (A) As the front gate voltage V_{fg} is increased, n_f rises for gate voltage $V_{fg} > -0.2\text{V}$ and $V_{fg} < -0.6\text{V}$, and n_b slightly decreases due to a negative compressibility [10]. (B) For

the front gate voltage $-0.6\text{V} < V_{\text{fg}} < -0.2\text{V}$ the electrons are not localized in individual wells but are resonating between them with the averaged densities n_s and n_a on the symmetric and antisymmetric states. The maximum density difference at $V_{\text{fg}} = -0.41\text{V}$ gives $\Delta_{\text{SAS}} \approx 6.8\text{K}$.

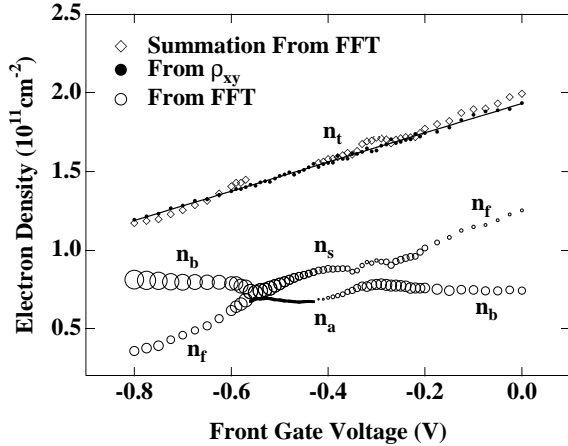


FIG. 1. Carrier density as a function of the front gate voltage. The open circles are the electron densities obtained from Fourier transforms of SdH signals. The total electron densities (solid circles) are measured by the low field Hall resistance. The size of the open circle is proportional to the signal intensity. The open square is the sum of electron densities. The solid curve in the density n_a is not observed by SdH but is calculated by $n_a = n_t - n_s$.

In Fig.2 we show the magneto- and Hall resistance at $V_{\text{bg}} = -37.2\text{V}$ under two typical V_{fg} . Balanced QH states are seen in Fig. 2(a) at $V_{\text{fg}} = -0.41\text{V}$, where $n_f/n_b = 1/1$. Unbalanced QH states are seen in Fig. 2(b) at $V_{\text{fg}} = -0.80\text{V}$, where $n_f/n_b \approx 1/2$.

Odd-integer QH states in the inset of Fig.2(a) are the monolayer states stabilized by the tunneling interaction. It exists only up to a certain magnetic field, beyond which bilayer QH states stabilized by the Coulomb interaction are expected to occur [1]. The $\nu = 1$ QH state, which is unstable at higher total electron density, has been stabilized at $n_t = 1.4 \times 10^{11}\text{ cm}^{-2}$. This property can be understood based on the phase diagram [1]. On the other hand, even-integer QH states will be bilayer states made of the same monolayer QH states localized in the two wells, which we call compound states with $(\nu_f, \nu_b) = (\nu/2, \nu/2)$, or the monolayer state stabilized by the tunneling interaction. We cannot distinguish them. They are present since these states are robust. The $\nu = 2/3$ state is the Ψ_{330} state which is a compound state with $(\nu_f, \nu_b) = (1/3, 1/3)$.

In Fig.2(b) we report the QH effect in the unbalanced configurations obtained by controlling the bias voltages. The $\nu = 3$ and 6 states are compound states with $(\nu_f, \nu_b) = (1, 2)$ and $(2, 4)$, respectively, where $\nu = \nu_f + \nu_b$ and $\nu_f/\nu_b = n_f/n_b$. The $\nu = 4$ and 8 states are the "tails"

of the compound states with $(\nu_f, \nu_b) = (1, 3)$ and $(2, 6)$ broadened by disorder in the sample, because the plateau became wider as the system approached $n_b/n_f = 1/3$. The origin of the $\nu = 1$ and $1/3$ state is discussed in the following stage.

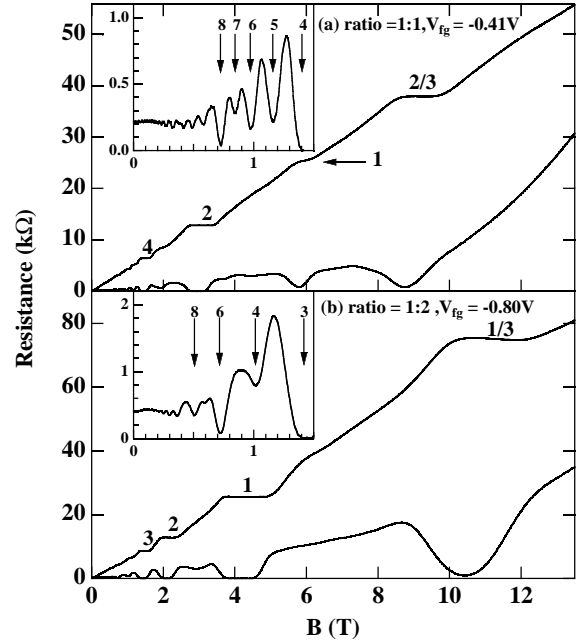


FIG. 2. Magneto and Hall resistance, ρ_{xx} and ρ_{xy} , for two typical density ratios n_f/n_b . The appearance of QH states depends critically on this ratio. In (a) $n_f = n_b = 6.9 \times 10^{10}\text{ cm}^{-2}$. In (b) $n_f = 3.4 \times 10^{10}\text{ cm}^{-2}$ and $n_b = 7.4 \times 10^{10}\text{ cm}^{-2}$.

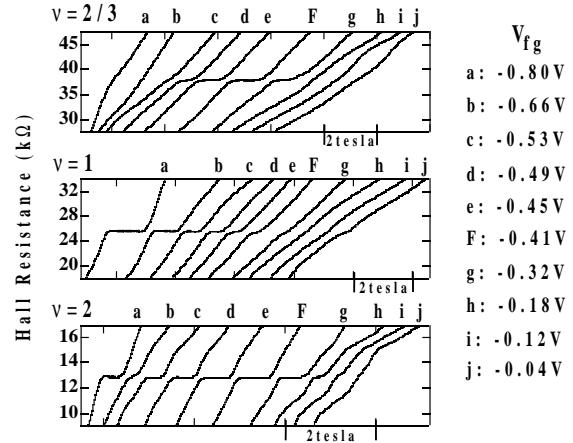


FIG. 3. The Hall resistances near the plateau of $\nu=2/3$, 1 and 2 QH state are shown at various V_{fg} . The curve (F) represents balanced QH effect.

In Fig.3 we give the Hall resistance measured at fixed $V_{\text{bg}} = -37.2\text{V}$ and various V_{fg} . It is customary to discuss the stability of the QH states by the value of the magnetoresistance (ρ_{xx}). We propose to discuss the stability in terms of the width of the Hall plateau. We have

defined the width of the Hall plateau by the width of the magnetic field within the $\pm 2.5\%$ range of the Hall resistance after subtracting the classical Hall resistance, as illustrated in Fig.4.

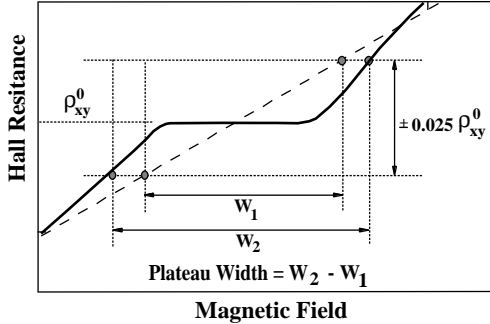


FIG. 4. The definition of the Hall plateau width. The dotted line represents a classical Hall resistance, and ρ_{xy}^0 is a quantized Hall resistance.

As is seen in Fig.5, the plateau widths of the $\nu = 2$ and $2/3$ state are widest when $n_f/n_b = 1$, and decrease monotonically as it deviates from the balanced point. This is explained by considering that the $\nu = 2$ and $2/3$ states are compound states with $(\nu_f, \nu_b) = (1, 1)$ and $(1/3, 1/3)$, respectively. The $\nu = 2$ data show an increase below $-0.7V$, and reaches a maximum at $-0.8V$ which is the edge of our experimental region. We interpret it as a tail of the monolayer state with $(\nu_f, \nu_b) = (0, 2)$. In the figure the behavior of the $\nu = 1$ QH state is strikingly different from all the other states. The state is stable over a wide range of density ratio, and at the same time no peak is observed at the balanced point. The QH state would be stablest at the balance point if it were stabilized by either Δ_{SAS} or any simple correlations.

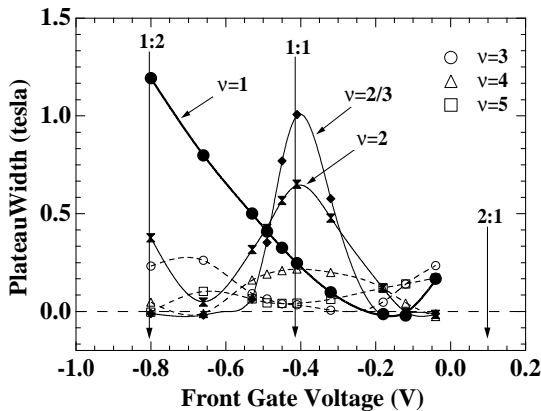


FIG. 5. The Hall plateau width as a function of the front gate voltage V_{fg} . The curved lines interpolate data points.

In Fig.6 the width of the Hall plateau of the $\nu = 1$ state is given as a function of n_t for four different back gate voltage V_{bg} . It is seen that the plateau width depends on the total density n_t but not on the density ratio, suggesting an interesting scaling law. The stabil-

ity decreases as n_t increases, and the QH state becomes unstable when $n_t \approx 1.7 \times 10^{11} \text{ cm}^{-2}$. As the density increases beyond $1.7 \times 10^{11} \text{ cm}^{-2}$, the $\nu = 1$ state becomes stable again. This increase is probably due to the tail of the compound state with $(\nu_f, \nu_b) = (2/3, 1/3)$ having the peak at $n_f/n_b = 2/1$.

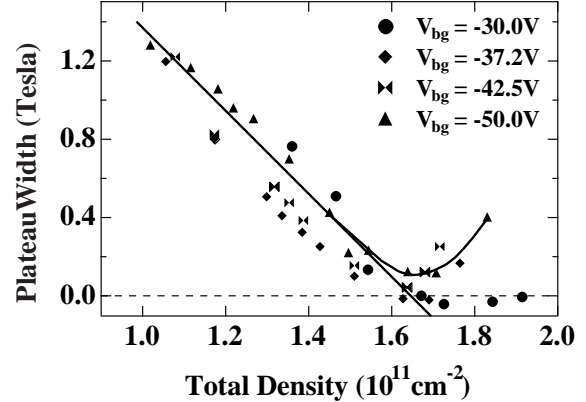


FIG. 6. Stability of $\nu = 1$ as a function of the total density. The dependence of the Hall plateau width on the total density is given for four different back gate voltage V_{bg} . Almost all data points are on a straight line below the density $1.6 \times 10^{11} \text{ cm}^{-2}$, and deviate from it by the tail of the $(\nu_f, \nu_b) = (2/3, 1/3)$ state.

III. INTERLAYER QUANTUM COHERENCE

In this section we discuss the origin of the peculiar property of the $\nu = 1$ QH state. We relate it to IQC based on the composite-boson picture [3,5,11].

In the bilayer system the Hamiltonian H is the sum of the kinetic term H_K , the Coulomb term H_C and the tunneling term H_T . (For simplicity we freeze the spin degree of freedom.) The Coulomb term may be written as a sum of two terms [11], $H_C = H_C^+ + H_C^-$, where H_C^+ depends only on the total electron density n_t while H_C^- depends only on the density difference $n_f - n_b$. The term H_C^- describes the capacitance energy stored between the two layers. The key behavior is that $H_C^- \rightarrow 0$ as $d/\ell_B \rightarrow 0$ and $H_C^- \rightarrow H_C^+$ as $d/\ell_B \rightarrow \infty$. The system has a rich phase diagram depending on relative strength of these interaction terms. We expect to have the following three phases (A) \sim (C).

When the capacitance term H_C^- is negligible, the bilayer system is mapped exactly to a monolayer system with the spin degree of freedom, where the tunneling term is mapped to the Zeeman term [6,11]. Therefore, we have two phases: (A) For a large Δ_{SAS} , the bilayer QH state is reduced to a "monolayer" QH state built on the symmetric or antisymmetric state. It is clear that the density ratio is fixed as $n_f/n_b = 1$ for the state to realize. (B) For a small Δ_{SAS} it is considered as a QH ferromagnet [6,11] identified with the Ψ_{mmm} state, about which we explain soon.

The capacitance term H_C^- acts to break these phases, yielding a new phase (C) described by the $\Psi_{m_f m_b m}$ state with $m_f m_b \neq m^2$. This phase realizes [3] at

$$\nu = \frac{m_f + m_b - 2m}{m_f m_b - m^2}, \quad (1)$$

where the density ratio is fixed as

$$\frac{n_f}{n_b} = \frac{m_b - m}{m_f - m}. \quad (2)$$

A special limit with $m = 0$ corresponds to the compound state with $(\nu_f, \nu_b) = (1/m_f, 1/m_b)$. It should be emphasized that the QH state exists only at a fixed density ratio in phases (A) and (C).

We now explain why phase (B) is peculiar. The nature of the QH ferromagnet is most easily revealed based on the composite-boson picture. The composite-boson field is defined with the aid of the Chern-Simons (CS) field. We first neglect the terms H_C^- and H_T in the Hamiltonian. Since the term H_C^+ does not discriminate electrons belonging to different layers, only one CS field \mathbf{C} is introduced. The CS flux is attached to each electron and determined by

$$\text{rot } \mathbf{C} = mn_t \phi_0, \quad (3)$$

in terms of the total density n_t and the Dirac flux unit $\phi_0 = 2\pi\hbar c/e$. Bose condensation occurs when the external magnetic field is cancelled by the CS field, $\mathbf{C} + \mathbf{A}^{\text{ext}} = 0$. The constraint (3) dictates that this is only possible at the filling factor

$$\nu = \frac{1}{m}. \quad (4)$$

The essential point is that *the density ratio n_f/n_b is arbitrary*. Namely, we obtain degenerate ground states $|\Delta n\rangle$ with arbitrary density difference $\Delta n = n_f - n_b$. The interlayer phase θ is the variable conjugate to Δn . The coherent states read

$$|\Psi(\theta)\rangle = \sum_{\Delta n} e^{-i\theta\Delta n} |\Delta n\rangle. \quad (5)$$

The coherent mode is a Goldstone mode. Although the degeneracy is removed by the capacitive term H_C^- and the tunneling term H_T , there are states having various density difference Δn and hence the coherent states (5) persist. The coherent mode is made gapful and called a pseudo-Goldstone mode. Various IQC phenomena are expected to occur on these states [3,5,6,11].

As we have explained, the condition for the emergence of IQC is the existence of QH states with arbitrary density difference Δn . In our data only the $\nu = 1$ QH state has a peculiar feature that it continues to exist over a wide range of Δn . Another characteristic feature of the $\nu = 1$ QH state is that the stability depends only on the total density and not on the density difference. This

is naturally explained in the composite-boson picture. Since the Ψ_{111} state is considered as an integer QH state made of electrons disregarding their layer dependence as in (3), the stability should not depend on the density difference. Furthermore, as the density becomes larger, the magnetic length ℓ_B becomes smaller. Since the ratio d/ℓ_B becomes larger, the interlayer Coulomb interaction becomes effectively smaller. It acts to break the Ψ_{111} state. Hence, the stability decreases as the total density increases, and the QH state breaks down eventually at a critical density.

In conclusion the best signal for the emergence of IQC is the existence of QH states $|\Delta n\rangle$ with various density difference Δn . We have observed these QH states in unbalanced double quantum wells by applying bias voltages to the system.

IV. ACKNOWLEDGEMENT

We thank T. Saku (NTT) for providing us the sample used in the present work, to K. Hirakawa and S. Kawakami for providing us samples used in the early stage, to O. Sakai and T. Nakajima for useful discussions, and M. Suzuki for technical assistance. This work was partly done at Laboratory for Electronic Intelligent Systems, Research Institute of Electrical Communication, Tohoku University. This work was supported by grants from the Ministry of Education, Science, Sports and Culture of Japan, and from Multi-disciplinary Science Foundation.

-
- [1] A.H. MacDonald, P.M. Platzmann and G.S. Boebinger, Phys. Rev. Lett. **65**, 775 (1990); S. He, S.D. Sarma and X.C. Xie, Phys. Rev. B **47**, 4394 (1993).
 - [2] Y.W. Suen, L.W. Engel, M.B. Santos, M. Shayegan, and D.C. Tsui, Phys. Rev. Lett. **68**, 1379 (1992); J.P. Eisenstein, G.S. Boebinger, L.N. Pfeiffer, K.W. West and Song He, Phys. Rev. Lett. **68**, 1383 (1992).
 - [3] Z.F. Ezawa and A. Iwazaki, Int. J. Mod. Phys. B **6**, 3205 (1992); Phys. Rev. B **47**, 7295 (1993); Phys. Rev. B **48**, 15189 (1993).
 - [4] S.Q. Murphy, J.P. Eisenstein, G.S. Boebinger, L.N. Pfeiffer and K.W. West, Phys. Rev. Lett. **72**, 728 (1994).
 - [5] Z.F. Ezawa, Phys. Rev. B **51**, 11152 (1995); Z.F. Ezawa and A. Iwazaki, Int. J. Mod. Phys. B **8**, 2111 (1994).
 - [6] K. Yang, K. Moon, L. Zheng, A.H. MacDonald, S.M. Girvin, D. Yoshioka and S.C. Zhang, Phys. Rev. Lett. **72**, 732 (1994); K. Moon, H. Mori, K. Yang, S.M. Girvin, A.H. MacDonald, L. Zheng, D. Yoshioka and S.C. Zhang, Phys. Rev. B **51**, 5138 (1995).
 - [7] G.S. Boebinger, H.W. Jiang, L.N. Pfeiffer and K.W. West, Phys. Rev. Lett. **64**, 1793 (1990).

- [8] T.S. Lay, Y.W. Suen, H.C. Manoharan, X. Ying, M.B. Santos and M. Shayegan, Phys. Rev. B **50**, 17725 (1994).
- [9] A.R. Hamilton, M.Y. Simmons and F.M. Bolton, N.K. Patel, I.S. Millard, J.T. Nicholls, D.A. Richie and M. Pepper, Phys. Rev. B **54**, R5259 (1996).
- [10] X. Ying, S.R. Parihar, H.C. Manoharan and M. Shayega, Phys. Rev. B **52**, 11611 (1995); N.K. Patel *et al.*, Phys. Rev. B **53**, 15443 (1996).
- [11] Z.F. Ezawa, Phys. Lett. A (to appear); Phys. Rev. B **55**, 7771 (1997).